

ERRATUM: “PROGENITOR-EXPLOSION CONNECTION AND REMNANT BIRTH MASSES FOR NEUTRINO-DRIVEN SUPERNOVAE OF IRON-CORE PROGENITORS” (2012, APJ, 757, 69)

THOMAS ERTL^{1,2}

AND

MARCELLA UGLIANO¹, HANS-THOMAS JANKA¹, ANDREAS MAREK¹, AND ALMUDENA ARCONES^{3,4}

An erroneous interpretation of the hydrodynamical results led to an incorrect determination of the fallback masses in Ugliano et al. (2012), which also (on a smaller level) affects the neutron star masses provided in that paper. This problem was already addressed and corrected in the follow-up works by Ertl et al. (2015) and Sukhbold et al. (2015). Therefore, the reader is advised to use the new data of the latter two publications. In the remaining text of this *Erratum* we present the differences of the old and new fallback results in detail and explain the origin of the mistake in the original analysis by Ugliano et al. (2012).

The fallback masses obtained by Ugliano et al. (2012) are displayed in Fig. 1 by white histogram bars. The red bars show the fallback masses determined for the same progenitor set with the improved explosion modeling of Ertl et al. (2015) and the same *incorrect* fallback criterion as applied by Ugliano et al. (2012). The results basically agree, and a tendency of higher fallback masses for lower-mass progenitors is present in both data sets. The quantitative differences are a consequence of improvements of some modeling aspects by Ertl et al. (2015). The blue histogram bars represent the fallback masses as determined with a *correct* evaluation of the fallback for the models of Ertl et al. (2015). The correct values are considerably smaller in particular for progenitors below $\sim 20 M_{\odot}$. The trend of increasing fallback masses for less massive stars is inverted to the opposite behavior.

The reason for the error in the fallback analysis by Ugliano et al. (2012) can be understood from the dynamics plotted in Fig. 2. After the subsiding of the neutrino-driven wind (on a time scale of 10–20 seconds after bounce), gas in the inner regions of the exploding star is decelerated by the gravitational pull of the neutron star and collapses back. This leads to fallback with a rate that peaks at some ten seconds post bounce and decreases afterwards according to a power law ($\propto t^{-5/3}$).

On a time scale of days to weeks, the reverse shock created when the supernova shock passes the helium-hydrogen interface, propagates toward the center of the exploding star. Moving backward through the inner layers of the star, the reverse shock accelerates the inward motion of the gas. At the same time it compresses and heats the shocked gas, raising its pressure by 2–3 orders of magnitude. When the reverse shock leaves the computational domain through the inner grid boundary, which is treated as an open (outflow) boundary with a radial location of typically 10^{10} cm during these late stages of the evolution, the gas in a large volume of the star has negative (supersonic) velocities (Fig. 2). Shortly afterwards, however, the inflow of the stellar matter is reversed and a strong outward moving shock develops.

Ugliano et al. (2012) calculated the fallback mass by taking at this “reflection time”, t_r , the sum of all gas mass that had fallen through the inner grid boundary until this time plus an estimate of additional fallback that will be added later from the mass that has been accelerated inward by the reverse shock. For this latter contribution they took the arithmetic average of the mass at time t_r with negative velocities and the mass with velocities smaller than the escape velocity v_{esc} (in all cases these two masses were nearly identical):

$$M_{\text{fb,err}} = \int_0^{t_r} dt \dot{M}_{\text{ib}}(t) + 0.5 [M_{v<0}(t_r) + M_{v<v_{\text{esc}}}(t_r)] . \quad (1)$$

The values of the fallback mass thus obtained are near the local, late-time maxima of the red lines in the upper two panels of Fig. 2. Applying this recipe, Ugliano et al. (2012) erroneously assumed that the dynamical evolution as computed for $t > t_r$ is not trustworthy, because they interpreted the outward going wave as a consequence of a reflection of the reverse shock at the inner grid boundary and therefore as a numerical artifact caused by the presence of this boundary.

A detailed, time-dependent analysis, however, reveals that this interpretation was not correct. Figure 2 shows what happens. The infall of the reverse-shock heated matter is decelerated because of the steepening of the negative pressure gradient that happens as the inward flow gets geometrically focussed. The deceleration produces a wave that begins to move outward again and steepens into a shock front when the expansion velocity exceeds the local sound speed. This happens well after the reverse shock has left the grid, at which time no numerical artifact is created (in fact, such an artifact would not be able to travel into the computed volume because the postshock flow streams to the boundary with supersonic speed). The “reflection wave” is therefore *not* a numerical artifact but a physics phenomenon, in which the contracting stellar mass itself reverses its infall. Tests with smaller radii for the location of the inner grid boundary (e.g., 5×10^8 cm or 10^9 cm) show exactly the same dynamical behavior, confirming this “self-reflection”. The correct evaluation of the fallback is therefore a simple time integral of the mass flow rate through the inner boundary:

$$M_{\text{fb,cor}} = \int_0^{\infty} dt \dot{M}_{\text{ib}}(t) . \quad (2)$$

This integration was applied by Ertl et al. (2015) and Sukhbold et al. (2015) and yields the values of the blue histogram bars in Fig. 1.

¹ Max-Planck-Institut für Astrophysik, Karl-Schwarzschild-Str. 1, 85748 Garching, Germany

² Physik Department, Technische Universität München, James-Frank-Straße 1, 85748 Garching, Germany

³ Institut für Kernphysik, Technische Universität Darmstadt, Schlossgartenstr. 2, 64289 Darmstadt, Germany

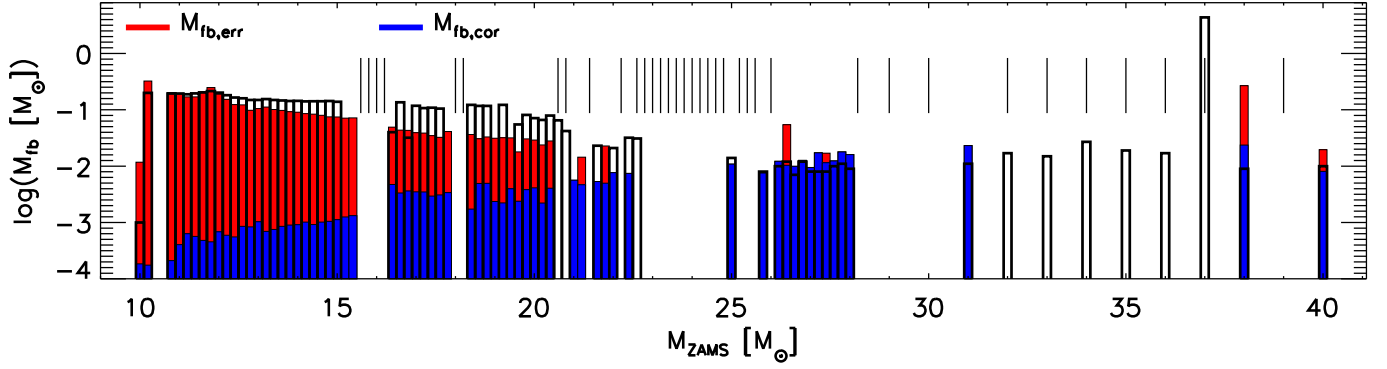


FIG. 1.— Fallback masses for all progenitors investigated by Ugliano et al. (2012). The white histogram bars display the results of Ugliano et al. (2012). The red bars show the results from simulations by Ertl et al. (2015) with modeling improvements in various aspects (but with the same $19.8 M_{\odot}$ red supergiant model for the SN 1987A calibration case), also applying the incorrect fallback estimate of Eq. (1). The blue histogram bars display the fallback masses as computed by Ertl et al. (2015) with the correct fallback determination according to Eq. (2). The vertical lines in the upper part of the plot indicate non-exploding cases obtained with the improved modeling by Ertl et al. (2015). Note that for better comparison with Ugliano et al. (2012) the models reported in this plot do *not* include the calibration of the low-mass explosions with the Crab-like progenitor introduced by Ertl et al. (2015) and Sukhbold et al. (2015).

REFERENCES

Ertl, T., Janka, H.-Th., Woosley, S. E., Sukhbold, T., and Ugliano, M. 2015, ApJ, in press; arXiv:1503.07522

Sukhbold, T., Ertl, T., Woosley, S. E., Brown, J. M., & Janka, H.-T. 2015, ApJ, submitted; arXiv:1510.04643

Ugliano, M., Janka, H.-T., Marek, A., & Arcones, A. 2012, ApJ, 757, 69

⁴ GSI Helmholtzzentrum für Schwerionenforschung GmbH, Planckstr. 1, 64291 Darmstadt, Germany

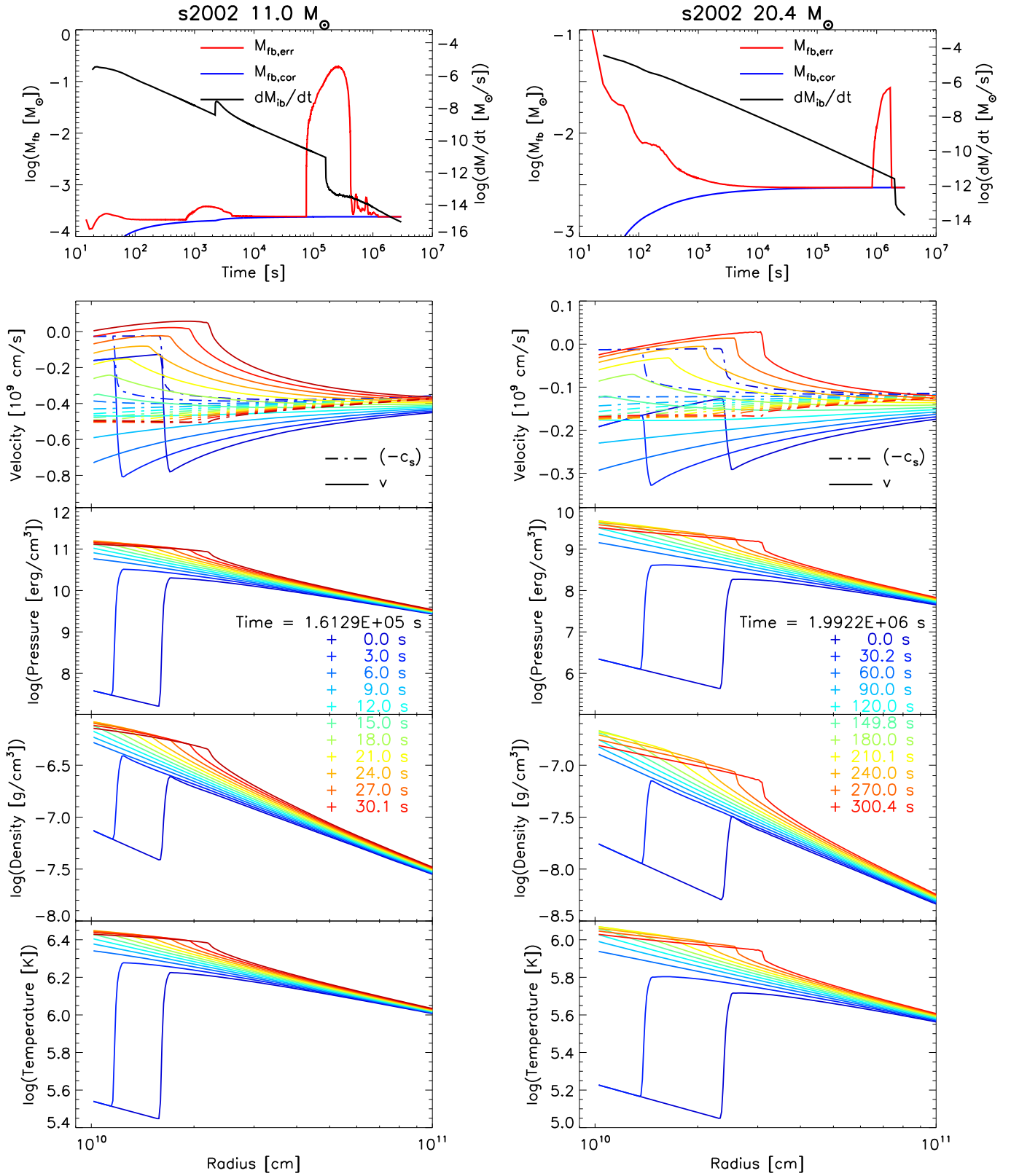


FIG. 2.— Fallback and dynamical evolution in two exemplary explosion simulations for an 11.0 M_{\odot} progenitor (left) and a 20.4 M_{\odot} case (right). The upper panels display the total fallback mass as function of time. The red line gives the incorrect result from applying the rhs of Eq. (1) at all times. The “reflection time”, t_r , is at about the instant of the late, local maximum of the red curve. The previous, incorrect estimate of the fallback mass (Eq. 1) corresponds to a value close to this maximum. The rising blue line shows the correct evaluation according to Eq. (2), the black line with the decaying trend the corresponding mass-accretion rate, \dot{M}_{fb} . The temporary increase of \dot{M}_{fb} in the 11.0 M_{\odot} model at ~ 2000 s is connected to the inward acceleration of matter by the first reverse shock that is created when the supernova shock passes the carbon-helium interface. The sets of lower panels display velocity (v ; solid lines) and adiabatic sound speed (c_s ; dash-dotted lines), pressure, density, and temperature profiles (from top to bottom) for selected instants around the “reflection time”.